First Direct Measurement of the Proton's Weak Charge

Androić, Darko; Armstrong, D. S.; Asaturyan, A.; Averett, T.; Balewski, J.; Bartlett, K.; Beaufait, J.; Beminiwattha, R. S.; Benesch, J.; Benmokhtar, F.; ...

Source / Izvornik: **European Physical Journal Web of Conferences, 2017, 137**

Conference paper / Rad u zborniku

Publication status / Verzija rada: **Published version / Objavljena verzija rada (izdavačev PDF)**

https://doi.org/10.1051/epjconf/201713708005

Permanent link / Trajna poveznica: https://urn.nsk.hr/urn:nbn:hr:217:487300

Rights / Prava: Attribution 4.0 International/Imenovanje 4.0 međunarodna

Download date / Datum preuzimanja: **2024-03-29**



Repository / Repozitorij:

Repository of the Faculty of Science - University of Zagreb





EPJ Web of Conferences **137**, 08005 (2017) DOI: 10.1051/epjconf/201713708005
XIIth Quark Confinement & the Hadron Spectrum

Q_{weak}: First Direct Measurement of the Proton's Weak Charge

D. Androic[1], D.S. Armstrong[2], A. Asaturyan[3], T. Averett[2], J. Balewski[4], K. Bartlett[2], J. Beaufait[5], R.S. Beminiwattha[6], J. Benesch[5], F. Benmokhtar[7], J. Birchall[8], R.D. Carlini[5,2], G.D. Cates[9], J.C. Cornejo[2], S. Covrig[5], M.M. Dalton[9], C.A. Davis[10], W. Deconinck[2], J. Diefenbach[11], J.F. Dowd[2], J.A. Dunne[12], D. Dutta[12], W.S. Duvall[a13], M. Elaasar[14], W.R. Falk[8], J.M. Finn[2], T. Forest[15,16], C. Gal[9], D. Gaskell[5], M.T.W. Gericke[8], J. Grames[5], V.M. Gray[2], K. Grimm[16,2], F. Guo[4], J.R. Hoskins[2], K. Johnston[16], D. Jones[9], M. Jones[5], R. Jones[17], M. Kargiantoulakis[9], P.M. King[6], E. Korkmaz[18], S. Kowalski[4], J. Leacock[13], J. Leckey[2], A.R. Lee[13], J.H. Lee[6,2], L. Lee[10,8], S. MacEwan[8], D. Mack[5], J.A. Magee[2], R. Mahurin[8], J. Mammei[13], J.W. Martin[19], M.J. McHugh[20], D. Meekins[5], J. Mei[5], R. Michaels[5], A. Micherdzinska[20], A. Mkrtchyan[3], H. Mkrtchyan[3], N. Morgan[13], K.E. Myers[20], A. Narayan[12], L.Z. Ndukum[12], V. Nelyubin[9], H. Nuhait[16], Nuruzzaman[11,12], W.T.H van Oers[10,8], A.K. Opper[20], S.A. Page[8], J. Pan[8], K.D. Paschke[9], S.K. Phillips[21], M.L. Pitt[13], M. Poelker[5], J.F. Rajotte[4], W.D. Ramsay[10,8], J. Roche[6], B. Sawatzky[5], T. Seva[1], M.H. Shabestari[12], R. Silwal[9], N. Simicevic[16], G.R. Smith[5], P. Solvignon[5], D.T. Spayde[22], A. Subedi[12], R. Subedi[20], R. Suleiman[5], V. Tadevosyan[3], W.A. Tobias[9], V. Tvaskis[19], B. Waidyawansa[6], P. Wang[8], S.P. Wells[16], S.A. Wood[5], S. Yang[2], R.D. Young[24], P. Zang[24], and S. Zhamkochyan[3]

[1] *University of Zagreb, Zagreb, HR 10002 Croatia*
[2] *College of William and Mary, Williamsburg, VA 23185 USA*
[3] *A. I. Alikhanyan National Science Laboratory (Yerevan Physics Institute), Yerevan 0036, Armenia*
[4] *Massachusetts Institute of Technology, Cambridge, MA 02139 USA*
[5] *Thomas Jefferson National Accelerator Facility, Newport News, VA 23606 USA*
[6] *Ohio University, Athens, OH 45701 USA*
[7] *Christopher Newport University, Newport News, VA 23606 USA*
[8] *University of Manitoba, Winnipeg, MB R3T2N2 Canada*
[9] *University of Virginia, Charlottesville, VA 22903 USA*
[10] *TRIUMF, Vancouver, BC V6T2A3 Canada*
[11] *Hampton University, Hampton, VA 23668 USA*
[12] *Mississippi State University, Mississippi State, MS 39762 USA*
[13] *Virginia Polytechnic Institute & State University, Blacksburg, VA 24061 USA*
[14] *Southern University at New Orleans, New Orleans, LA 70126 USA*
[15] *Idaho State University, Pocatello, ID 83209 USA*
[16] *Louisiana Tech University, Ruston, LA 71272 USA*
[17] *University of Connecticut, Storrs-Mansfield, CT 06269 USA*
[18] *University of Northern British Columbia, Prince George, BC V2N4Z9 Canada*
[19] *University of Winnipeg, Winnipeg, MB R3B2E9 Canada*
[20] *George Washington University, Washington, DC 20052 USA*
[21] *University of New Hampshire, Durham, NH 03824 USA*
[22] *Hendrix College, Conway, AR 72032 USA*
[23] *University of Adelaide, Adelaide, SA 5005 Australia*
[24] *Syracuse University, Syracuse, NY 13210 USA*

[a] e-mail: wsduvall@vt.edu

© The Authors, published by EDP Sciences. This is an open access article distributed under the terms of the Creative Commons Attribution License 4.0 (http://creativecommons.org/licenses/by/4.0/).

Abstract. The $Q_{\rm weak}$ experiment, which took data at Jefferson Lab in the period 2010 - 2012, will precisely determine the weak charge of the proton by measuring the parity-violating asymmetry in elastic e-p scattering at 1.1 GeV using a longitudinally polarized electron beam and a liquid hydrogen target at a low momentum transfer of $Q^2 = 0.025\,(\mathrm{GeV/c})^2$. The weak charge of the proton is predicted by the Standard Model and any significant deviation would indicate physics beyond the Standard Model. The technical challenges and experimental apparatus for measuring the weak charge of the proton will be discussed, as well as the method of extracting the weak charge of the proton. The results from a small subset of the data, that has been published, will also be presented. Furthermore an update will be given of the current status of the data analysis.

1 Introduction

The $Q_{\rm weak}$ experiment [1] will precisely determine the weak charge of the proton $Q_{\rm W}^p$ by measuring the parity-violating asymmetry in elastic electron-proton scattering at a low momentum transfer of $Q^2 = 0.025\,(\mathrm{GeV/c})^2$. The weak charge of the proton is the neutral-weak analog of the proton's electric charge. While the results presented here only use the commissioning data, which is about 4% of the entire data set, the low Q^2 and use of the world parity violating electron scattering (PVES) data to constrain hadronic effects makes this the first direct measurement of $Q_{\rm W}^p$.

$Q_{\rm weak}$ ran in Hall C at the Thomas Jefferson National Accelerator Facility during the period 2010 - 2012. A 180 μA beam of longitudinally polarized electrons at 1.115 GeV scattered off a liquid hydrogen target of unpolarized protons. The scattered electrons were collimated in a scattering angle range of $\sim 6°$-$12°$ and then focused by a magnetic spectrometer onto quartz Čerenkov detector bars.

The experiment measures the parity-violating asymmetry by taking the difference of the elastic e-p scattering cross section for the two helicity states divided by the sum

$$A_{ep} = \frac{\sigma_+ - \sigma_-}{\sigma_+ + \sigma_-} \tag{1}$$

The asymmetry can be expressed at tree level in terms of electromagnetic, weak, and axial form factors as:

$$A_{ep} = \left[\frac{-G_F Q^2}{4\pi\alpha\sqrt{2}}\right]\left[\frac{\varepsilon G_E^\gamma G_E^Z + \tau G_M^\gamma G_M^Z - (1-4\sin^2\theta_W)\varepsilon' G_M^\gamma G_A^Z}{\varepsilon (G_E^\gamma)^2 + \tau (G_M^\gamma)^2}\right] \tag{2}$$

where

$$\varepsilon = \frac{1}{1+2(1+\tau)\tan^2\frac{\theta}{2}}, \quad \varepsilon' = \sqrt{\tau(1+\tau)(1-\varepsilon^2)} \tag{3}$$

are kinematic quantities, G_F is the Fermi constant, $\sin^2\theta_W$ is the weak mixing angle, $-Q^2$ is the four-momentum transfer squared, $\tau = Q^2/4M^2$ where M is the proton mass, and θ is the laboratory electron scattering angle. The explicit dependence on the proton's weak charge can be shown by rewriting [2] Eq. 2 as

$$A_{ep}/A_0 = Q_W^p + Q^2 B(Q^2,\theta), \quad A_0 = \left[\frac{-G_F Q^2}{4\pi\alpha\sqrt{2}}\right] \tag{4}$$

where $Q_{\rm W}^p$ is the intercept, and the hadronic form factors are contained in $B(Q^2,\theta)$, which can be extracted by doing a global analysis of all existing PVES data.

2 Experiment

The Q_{weak} apparatus, shown in Fig. 1, was constructed in Hall C at Jefferson Lab [3] [4]. It features

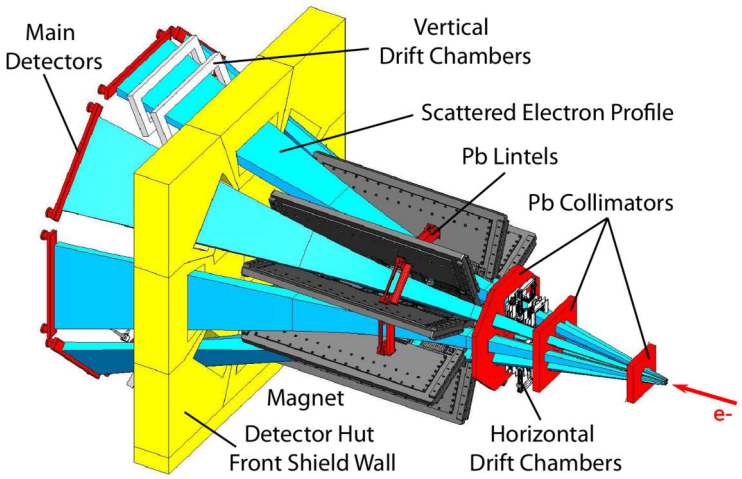


Figure 1. The Q_{weak} apparatus with lead collimators, horizontal drift chambers, lead lintels, spectrometer magnet, shield wall, vertical drift chambers and quartz main detector bar. Also shown is the scattered elastic electron path.

a ~ 35 cm long liquid hydrogen target, three lead collimators which define the acceptance, a toroidal magnet which focuses elastic electrons on the main detector bars as well as removes inelastically scattered electrons, and eight quartz Čerenkov main detector bars with azimuthal symmetry. Two sets of retractable vertical wire drift chambers and two sets of retractable horizontal wire drift chambers were used to characterize the Q^2 of the experiment. The main detector bars and drift chambers were protected by a large shield wall.

During the commissioning period, upon which the results presented here are based, Q_{weak} took 1.115 GeV electrons at a beam current of between 145 and 180 μA and a longitudinal polarization of 89% ± 1.8%. The scattering angle acceptance was 7.9° ± 3°, with an azimuthal acceptance of almost half of 2π. The Q^2 was determined to be 0.0250 ± 0.0006 (GeV/c)^2 from simulation [1].

2.1 Target

Q_{weak} had a liquid hydrogen target [3] that was designed to have very high power (more than 2100 W at 180 μA beam current) and have very low noise from target density fluctuations (less than 50 ppm noise). The target used a 34.5 cm long aluminum cell and thin entrance (0.10 mm) and exit (0.13 mm) windows. A centrifugal pump circulated the LH_2 though a closed loop and transversely across the beam. The closed loop also contained a 3 kW resistive heater to prevent the LH_2 from freezing when there is no beam and a 3 kW counterflow heat exchanger which used both 14 K helium coolant supplied to experiments as well as 4 K helium coolant provided by the accelerator. Designing a high power target while also minimizing noise from target boiling was achieved by using computational fluid dynamics to determine the optimal geometry which limited boiling along the beam axis and especially near the target windows. The measured density fluctuations were only 37 ± 5 ppm with 169 μA of beam rastered to a spot 4x4 mm^2 at the entrance to the target cell, and the target pump running at is nominal 28.5 Hz. This represented a very small part of the overall 236 ppm asymmetry width at this beam current.

2.2 Detectors

Q_{weak} used a ring of eight azimuthally symmetric synthetic quartz Čerenkov detectors [3]. The ring was placed 12.2 m downstream of the target and had a radius of 3.4 m. Azimuthal symmetry helped to reduce sensitivity to helicity correlated beam motion and residual transverse polarization. Each 2 m long bar was made by glueing together two 1 m long quartz bars end-to-end using optical compound. The final bar was 2 m x 18 cm x 1.25 cm. In order to reduce low energy backgrounds and boost gain, a 2 cm lead preradiator was placed in front of the quartz bar. Two quartz light guides were placed at each end of the quartz bar and were connected to 12.7 cm low gain PMTs. The PMTs current was put into a custom low noise I-to-V preamplifier and then into a ASIC low noise 18 bit ADC which sampled at 500 Hz. When operating with drift chambers inserted, high gain bases were used on the PMTs to accommodate the lower operating beam current.

2.3 Polarimetry

A very precise measurement of the polarization was required for Q_{weak} to achieve its precision goals. In order to achieve the stated goal of 1% two polarimeters were used. The first was the preexisting Hall C Møller polarimeter [5]. This polarimeter used a fully polarized iron foil with known analyzing power in a superconducting magnet to determine polarization at the percent level. This polarimeter only worked at low beam currents and disrupted data taking, therefore a Compton polarimeter was built in Hall C to provide a constant, non-invasive measurement of polarization to complement the Møller polarimeter. The Compton polarimeter used a circularly polarized laser in a cavity to provide a known analysing power [6]. Both the scattered electron and scattered photon were independently measured. Agreement between both polarimeters was within errors [3].

3 Analysis

The experimental asymmetry was constructed from beam charge normalized integrated detector current yields as

$$A_{raw} = \frac{Y^+ - Y^-}{Y^+ + Y^-} \tag{5}$$

for randomized helicity states. For this data set $A_{raw} = -169 \pm 31$ ppm [1]. Corrections for helicity correlated beam properties, non-linearity and transverse polarization were also made as

$$A_{msr} = A_{raw} + A_T + A_L - \sum_i \frac{\partial A}{\partial \chi_i} \Delta\chi_i \tag{6}$$

$$= A_{raw} + A_T + A_L + A_{reg} \tag{7}$$

where A_T is the residual transverse asymmetry, A_L is the non-linearity correction and A_{reg} is the regression correction for helicity correlated beam properties. There were also several backgrounds which need to be corrected for using measurements of the background asymmetry A_i and dilution f_i. The backgrounds in Q_{weak} came from aluminum target windows, beamline, soft neutrals, and inelastic events. The largest background was the aluminum target windows with an asymmetry of 1.76 ppm and a dilution of 3.2%. The final asymmetry was computed as

$$A_{ep} = R_{tot} \frac{\frac{A_{msr}}{P} - \sum_i f_i A_i}{1 - \sum_i f_i} \tag{8}$$

where R_{tot} includes radiative corrections, non-uniform light and Q^2 distribution on the detector bars, and uncertainties in Q^2 determination resulting in $R_{tot} = 0.98$. P is the measured polarization of 0.890 ± 0.018. The final value for $A_{ep} = -279 \pm 35$ (stat) $\pm$ 31 (sys) ppb.

3.1 Status of analysis towards the final result

Analysis of the full Q_{weak} data set is nearly complete including refined treatments of all major systematic errors. Here we describe one important systematic effect that is receiving careful attention. It is due to a double scattering effect from secondary scattering of the primary scattered electrons in the lead preradiators in front of the quartz main detectors. As scattered electrons pass through the spectrometer magnet, the initially purely longitudinally polarized electrons acquire $\sim 50\%$ transverse polarization by spin precession in the spectrometer magnet as shown in Fig. 2. When the electron

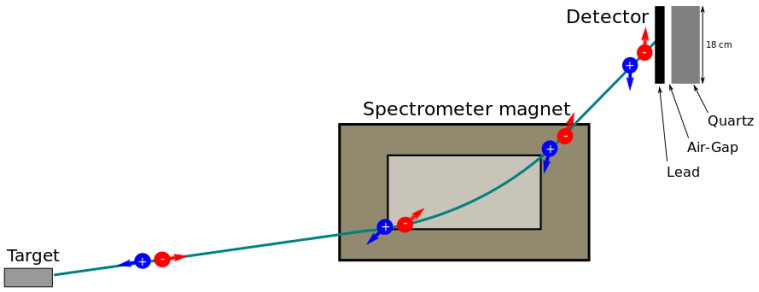


Figure 2. Scattered electrons with longitudinal polarization pass though the spectrometer magnet and pick up some transverse polarization before interacting with the lead preradiator.

interacts with the 2 cm lead preradiator in front of the detector bar, the transverse polarization combined with the parity-conserving left-right analyzing power in the scattering on lead gives rise to an asymmetry that is similar in magnitude but opposite in sign for the photomulitplier tubes attached to the left and right sides of a bar. Labeling the two PMTs on the bar as (+) and (-), this results in a non-zero *double difference* between the left and right PMT asymmetries on a bar:

$$A_{DD} = A_- - A_+ \tag{9}$$

The parity-violating asymmetry measured by a bar comes from averaging the left and right PMT asymmetries:

$$A_{PV} = \frac{A_- + A_+}{2} \tag{10}$$

While this double scattering effect cancels to first order for a perfect detector, broken symmetry in the detector bar can cause a small bias and therefore only partial cancellation. How well this asymmetry cancels is currently being studied using a Geant4 simulation benchmarked with measured light collection profiles for each individual bar and measured scattered fluxes incident on the detectors. Each of the eight bars has slightly different as-built properties, so we anticipate that a separate correction will be made for each. Analysis is currently focused on reducing the uncertainty on this correction.

4 Results

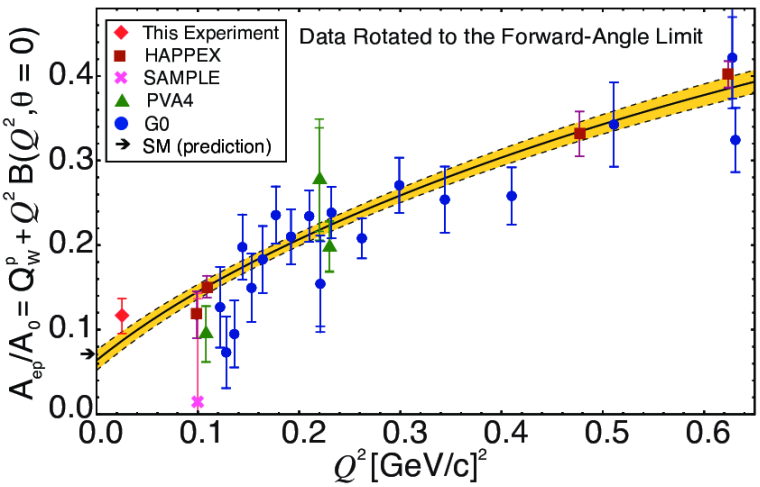


Figure 3. Global fit result presented in the forward angle limit calculated from the world PVES data as well as the recently published Q_{weak} [1] result (red point) based on 4% of the data. The yellow shaded area is the uncertainty of the fit. Individual point error bars are inflated slightly by rotation into the forward angle limit.

A global analysis using the recently published Qweak result (based on 4% of the data) [1], all PVES data [7–18] on hydrogen, deuterium and helium up to 0.63 GeV^2 was used to extract Q^p_{W} . The global fit prescription is discussed in depth in [2]. The global fit was done over five parameters: the quark weak charges C_{1u} and C_{1d}, the strange charge radius ρ_s and magnetic moment μ_s, and the isovector axial form factor $G_A^{Z(T=1)}$, which is constrained by theory. There was also a correction for the γ-Z box electroweak radiative correction based on the calculation in [19] and applied using prescription [20] using form factors from [21]. To illustrate this fit in two dimensions, θ dependence was removed using Eq. 2 and divided by A_0 given in Eq. 4. Projecting to $Q^2 = 0$ gives Q^p_W (PVES) = 0.064 ± 0.012.

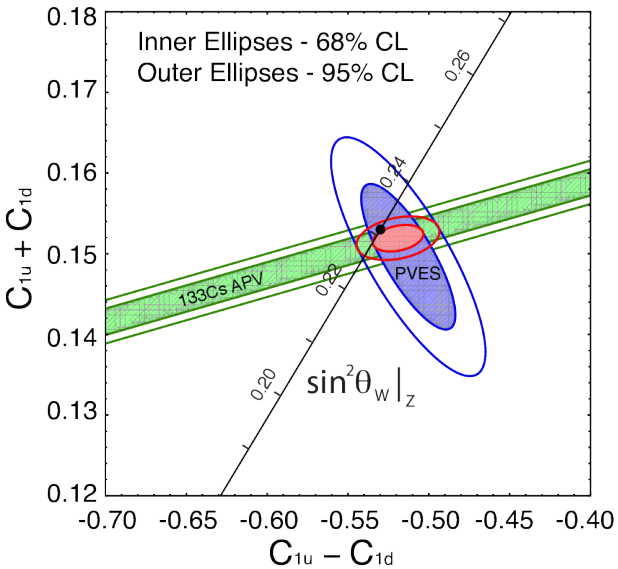


Figure 4. Constraints on the isovector ($C_{1u} - C_{1d}$) and isoscalar ($C_{1u} + C_{1d}$) quark weak coupling constants. The green APV band constrains the isoscalar combinations from ^{133}Cs. The blue ellipse represents the global fit of PVES data. Here the PVES data includes the recently published Qweak [1] result based on 4% of the data. The red ellipse shows the result from the combination of APV and PVES data. The black line represents the SM predicted value as a fuction of $\sin^2\theta_W$. The SM best fit value is represented by the black dot at $\sin^2\theta_W = 0.23116$.

Combining the Q_{weak} measurement of the proton weak charge with atomic parity violating (APV) data, it is possible to extract the weak charges of the quarks. Using precise measurements of the weak charge of ^{133}Cs [22] with atomic corrections [23] gives $C_{1u} = -0.1835 \pm 0.0054$ and $C_{1d} = 0.3355 \pm 0.0050$ with correlation coefficent of -0.980. These can be combined to give the weak charge of the neutron, Q_W^n (PVES+APV) $= -0.975 \pm 0.010$. Both the proton and neutron weak charges agree with the standard model values [24], Q_W^p (SM) $= 0.0710 \pm 0.0007$ and Q_W^n (SM) $= -0.9890 \pm 0.0007$.

At tree level in the Standard Model, the proton's weak charge is given by $Q_{\text{W}}^p = 1 - 4\sin^2\theta_W$. After electroweak radiative corrections are included in this expression, an effective weak mixing angle can be extracted from the measurement. A convenient way of comparing this measurement with other weak mixing angle measurements at a range of energy scales is the running plot shown in Figure 5.

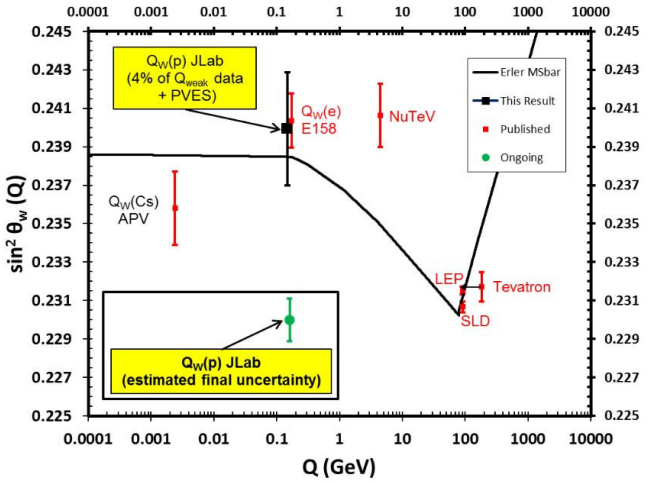


Figure 5. The calculated running of the weak mixing angle in the Standard Model, as defined in the modified minimal subtraction scheme, is shown as the solid line. The red data points are from published results: atomic parity violation (APV), parity-violating Møller scattering (SLAC E158), deep inelastic neutrino-nucleus scattering (NuTeV), and the Z-pole measurements at LEP and SLC. The black data point shows the recently published Q_{weak} experiment result based on 4% of the data, and the green point shows the estimated final uncertainty from the Q_{weak} experiment.

The commissioning results reported here are derived from only about 4% of the data that were collected for the full experiment. The final proton weak charge result extracted using the full dataset will be available in mid-2017.

Acknowledgements

The Q_{weak} experiment is supported in part by the US DOE, NSF, NSERC (Canada), Jefferson Laboratory, and TRIUMF.

References

[1] D. Androic et al. (Qweak), Phys. Rev. Lett. **111**, 141803 (2013)
[2] R.D. Young, R.D. Carlini, A.W. Thomas, J. Roche, Phys. Rev. Lett. **99**, 122003 (2007)
[3] T. Allison et al. (Qweak), Nucl. Instrum. Meth. **A781**, 105 (2015)
[4] D.S. Armstrong et al. (2012), 1202.1255
[5] M. Hauger et al., Nucl. Instrum. Meth. **A462**, 382 (2001)
[6] A. Narayan et al., Phys. Rev. **X6**, 011013 (2016)
[7] D.T. Spayde et al. (SAMPLE), Phys. Lett. **B583**, 79 (2004)
[8] T.M. Ito et al. (SAMPLE), Phys. Rev. Lett. **92**, 102003 (2004)

[9] K.A. Aniol et al. (HAPPEX), Phys. Rev. Lett. **82**, 1096 (1999)
[10] K.A. Aniol et al. (HAPPEX), Phys. Rev. Lett. **96**, 022003 (2006)
[11] K.A. Aniol et al. (HAPPEX), Phys. Lett. **B635**, 275 (2006)
[12] A. Acha et al. (HAPPEX), Phys. Rev. Lett. **98**, 032301 (2007)
[13] Z. Ahmed et al. (HAPPEX), Phys. Rev. Lett. **108**, 102001 (2012)
[14] D.S. Armstrong et al. (G0), Phys. Rev. Lett. **95**, 092001 (2005)
[15] D. Androic et al. (G0), Phys. Rev. Lett. **104**, 012001 (2010)
[16] F.E. Maas et al. (A4), Phys. Rev. Lett. **93**, 022002 (2004)
[17] F.E. Maas et al., Phys. Rev. Lett. **94**, 152001 (2005)
[18] S. Baunack et al., Phys. Rev. Lett. **102**, 151803 (2009)
[19] N.L. Hall, P.G. Blunden, W. Melnitchouk, A.W. Thomas, R.D. Young, Phys. Rev. **D88**, 013011 (2013), 1304.7877
[20] M. Gorchtein, C.J. Horowitz, M.J. Ramsey-Musolf, Phys. Rev. **C84**, 015502 (2011), 1102.3910
[21] J.J. Kelly, Phys. Rev. **C70**, 068202 (2004)
[22] C.S. Wood, S.C. Bennett, D. Cho, B.P. Masterson, J.L. Roberts, C.E. Tanner, C.E. Wieman, Science **275**, 1759 (1997)
[23] V.A. Dzuba, J.C. Berengut, V.V. Flambaum, B. Roberts, Phys. Rev. Lett. **109**, 203003 (2012)
[24] J. Beringer et al. (Particle Data Group), Phys. Rev. **D86**, 010001 (2012)